

# Influence of Environmental Conditions on Steel Corrosion in Concrete Exposed to Gamma Radiation <sup>†</sup>

Mariusz Dąbrowski <sup>1,\*</sup>, Justyna Kuziak <sup>2</sup>, Kinga Dziedzic <sup>1</sup> and Michał A. Glinicki <sup>1</sup>

<sup>1</sup> Institute of Fundamental Technological Research, Polish Academy of Sciences, Pawińskiego 5b, 02-106 Warsaw, Poland

<sup>2</sup> Department of Building Materials Engineering, Warsaw University of Technology, al. Armii Ludowej 16, 00-637 Warsaw, Poland

\* Correspondence: mdabrow@ippt.pan.pl

<sup>†</sup> Presented at the 10th MATBUD'2023 Scientific-Technical Conference "Building Materials Engineering and Innovative Sustainable Materials", Cracow, Poland, 19–21 April 2023.

**Abstract:** This article examines the problem of the service life of reinforced concrete structures intended for nuclear power plants and radiation waste storage bunkers when exposed to radiation. This research focused on assessing the corrosion resistance of steel bars under conditions of simultaneous exposure to gamma radiation and various environmental conditions affecting the rate of carbonation. Electrochemical measurements of steel bars were carried out on samples in three environmental conditions: in a laboratory–dry; enclosed in a can at RH = 50%; and enclosed in a can at RH = 100%. The durability of the passivation layer of steel on non-irradiated and irradiated specimens after 8 months of exposure to gamma radiation was compared. A lower degradation effect of gamma radiation was visible in fully water-saturated specimens.

**Keywords:** corrosion of steel; relative humidity variability; carbonation condition; EIS; polarization curve



**Citation:** Dąbrowski, M.; Kuziak, J.; Dziedzic, K.; Glinicki, M.A. Influence of Environmental Conditions on Steel Corrosion in Concrete Exposed to Gamma Radiation. *Mater. Proc.* **2023**, *13*, 44. <https://doi.org/10.3390/materproc2023013044>

Academic Editors: Katarzyna Mróz, Tomasz Tracz, Tomasz Zdeb and Izabela Hager

Published: 13 March 2023



**Copyright:** © 2023 by the authors. Licensee MDPI, Basel, Switzerland. This article is an open access article distributed under the terms and conditions of the Creative Commons Attribution (CC BY) license (<https://creativecommons.org/licenses/by/4.0/>).

## 1. Introduction

The durability of nuclear power plant constructions, with a service life of 30 years or more, is a desirable feature affecting electricity prices [1]. The corrosion of steel in concrete structures exposed to irradiation is one of the important parameters determining the long term suitability of the structure for further operation [2]. The structural properties of existing and new nuclear power plant buildings should be well established in terms of the expected period of operation.

The irradiation-induced aging of concrete in nuclear power plants, occurring over a long period of time in nuclear environments, should be considered. Common knowledge concerning the influence of gamma radiation shows that a significant deterioration of mechanical properties of concrete occurs when the gamma dose exceeds the threshold of  $1 \times 10^8$  Gy [3]. However, there are studies that report the deterioration of concrete properties resulting just from a few MGy of gamma radiation [4–6], especially in the early stage of hardening [7,8]. For the reinforced concrete structures of a nuclear power plant, the impact of CO<sub>2</sub> from the atmosphere is very important. Researchers confirm that the main product of carbonation is the formation of calcite and vaterite [9–11] and have suggested an increase in the rate of the carbonation reaction. Normally, reinforcing bars surrounded by concrete exist in high pH (around 13 for Portland cement) conditions, and such an alkaline environment protects against steel corrosion and the further deterioration of the structure. The acceleration of carbonation lowers the pH of the concrete and consequently leads to steel depassivation [12,13]. In addition, gamma radiation causes the decomposition of the aqueous pore solution near the steel reinforcing bars and the formation of oxidizing and reducing compounds [14], which can affect the properties of the passivation layer on

the steel surface. Investigations into gamma radiation on corrosion of metals and alloys are generally measured in water solution systems, simulating cement matrix conditions. Studies [15,16] conducted on different types of steel and alloys (AISI 304, carbon steel) and gamma radiation doses (range from 75 kGy to 3 MGy) did not provide a consistent answer regarding the effect of irradiation on steel corrosion. In the case of real cement-based composite systems, the low dose (300 kGy) of gamma radiation [17] does not change the properties of the steel protective layer. A dose of up to 2 MGy, as seen in previous research [18], demonstrated the effect of gamma radiation on the reduction of the protective properties of the passive layer of steel in mortar, located in a sealed can with CO<sub>2</sub> and medium relative humidity (RH = 50%). The effect has not been unequivocally confirmed, due to a lack of studies that have conducted measurements in strong radiation fields. A marginal number of papers (as reported in review paper [12]) consider the influence of humidity conditions on the passivation of steel in gamma radiation field. Humidity conditions are of key importance for the intensity of concrete carbonation [9] and, consequently, for the conditions of the reinforcement steel.

This research is a continuation of considerations concerning the effects of gamma radiation on steel corrosion in cement-based materials [18]. The main purpose of this research is to assess the effect of gamma radiation on reinforcing steel in humid conditions that favour concrete carbonation (approximately RH = 50%) and inhibit carbonation (RH = 100%). The potentiodynamic and electrochemical impedance spectroscopy measurements were used to assess the susceptibility of the steel to corrosion.

## 2. Experimental Program

### 2.1. Materials and Specimens

A mortar mix with Portland cement CEM I 52.5R [19] and quartz sand [20] was prepared. A total of 400 g of cement (density 3.1 kg/dm<sup>3</sup> and 4500 cm<sup>2</sup>/g Blaine specific surface) and 1350 g of sand was used. The w/c was 0.6. The cement mortar component proportions ensured an increase in open porosity and prevented the segregation of composition.

The specimens with the steel rebar were cast. The steel rebars, S235JR, with a diameter of 6 mm (according to EN 10025-2 [21]) were used. The chemical composition of steel, as declared by the producer, was given in [18]. Wet polishing with SiC paper (4000 grit) followed by sonication was performed before the steel bars were coated with epoxy resin. For each bar, 10 cm<sup>2</sup> of smooth steel surface was left for electrochemical measurements, according to PN-86-B-01810 [22]. Standard curing conditions before irradiation were used (temperature of 20 ± 2 °C, duration 28 days).

### 2.2. Specimen Conditioning and Gamma Radiation Exposure

Cylindrical mortar specimens with central placed steel rod were divided into three groups after curing time: the first was to be irradiated and second and third to be stored in the laboratory without irradiation. The two groups of specimens were placed in steel cans, as shown in Figure 1a. The third group was conditioned without canning. Subsequently, each group of specimens was placed in a CTS climate-controlled chamber (65% RH and CO<sub>2</sub> concentration of 1% in the air). Specimens were conditioned in open cans in the climate chamber for 24 h and then the cans were closed. The environmental conditions in the cans were designed for two RH—fully water-saturated condition and RH = 50 ± 5% (controlled by superabsorbent polymer). The third group of specimens, after 24 h of conditioning without a can, was cured under laboratory conditions (23 ± 1 °C and RH = 43 ± 5%).

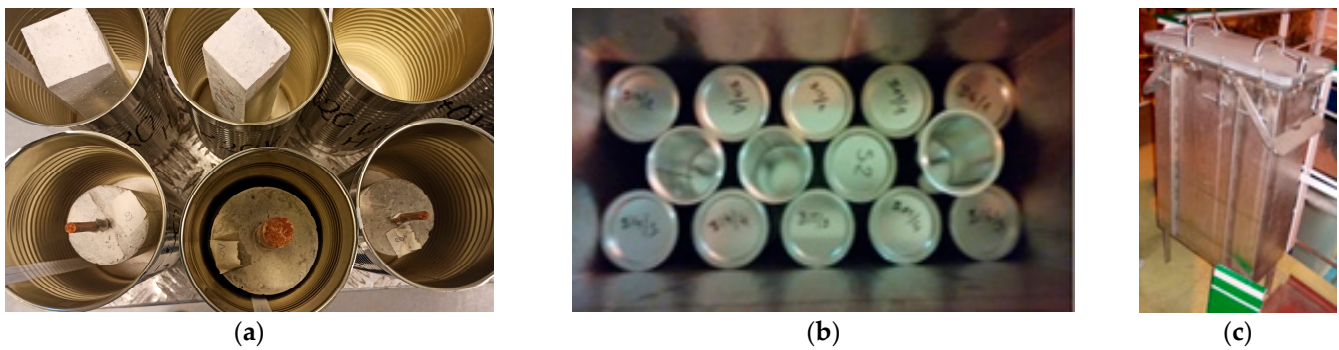


**Figure 1.** Location of specimens in the cans, (a) the arrangement of sealed cans (b), and the view of the prismatic steel box (c) immersed in the reactor pool close to spent nuclear fuel rods.

The research reactor of National Centre for Nuclear Research was used for the gamma irradiation of specimens sealed in cans and set in a prismatic steel box (Figure 1) in a manner described in detail in [18]. The absorbed dose was determined as the average value of two dosimeters attached to the walls of the cans. The dose of gamma radiation absorbed by the samples was close to 1.8 MGy. The specimens in the nuclear reactor-spent fuel pool were irradiated for 8 months. The second group of canned specimens was stored in climatic chamber at 38 °C without irradiation for the same period. The temperature in the climatic chamber corresponds with the temperature of irradiation specimen conditions. The measurements of environmental conditions (temperature and humidity) in closed cans confirmed the correctness of the adopted conditions. The results of mortar carbonation are presented and discussed in the research of Józwiak-Niedźwiedzka et al. [23].

### 2.3. Test Methods

The corrosion behaviour of steel in mortar was evaluated by electrochemical measurement (EIS and anodic polarization curves) using a potentiostat/galvanostat Autolab PGSTAT 302N with Nova 2.1 software. A three-electrode system consisted of reinforcement steel (the working electrode), saturated calomel electrode (SCE; the reference electrode), and a stainless-steel plate (counter electrode) was used. Measurements were taken at a temperature of  $20 \pm 1$  °C after 24 h of conditioning in a saturated solution of  $\text{Ca}(\text{OH})_2$  in water.

The EIS measurements settings:

- frequency range of  $5 \times 10^5$ – $5 \times 10^{-1}$  Hz;
- amplitude of the sine wave perturbation—10 mV.

The equivalent circuit (Figure 2) for the analysis of the obtained EIS spectra was chosen under the assumptions described in a previous study [18]. The following parameters were determined on the basis of the measurements:

- $R_{\text{pas}}$ —the ohmic resistance in the defects of passive layer;
- $R_{\text{ct}}$ —the charge transfer resistance;
- $Y_n$ —parameters of a constant phase element ( $\text{CPE}_m$ —mortar constant phase element;  $\text{CPE}_{\text{pas}}$ —passive surface constant phase element;  $\text{CPE}_{\text{dl}}$ —double layer on the steel constant phase element).

The EIS measurement was followed by an anodic polarization curve measurement. The settings for polarization measurements were as follows:

- potential range from  $-100$  mV, with respect to the corrosion potential, to  $800$  mV, with respect to the reference electrode,
- rate of potential change— $1$  mV/s.
- Parameters determined based on the recorded polarization curve:
  - $E_{\text{cor}}$ —corrosion potential,
  - $E_p$ —passivation potential,

- $E_{tr}$ —transpassivation potential,
- $j_{cor}$ —corrosion current density,
- $j_p$ —passivation current density.

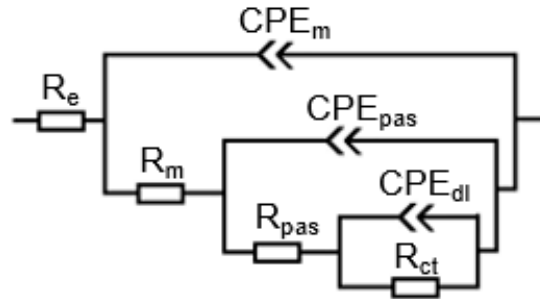


**Figure 2.** Equivalent circuit for steel in cement mortar ( $R_e$ —the electrolyte resistance;  $R_m$ —mortar resistance;  $CPE_m$ —constant phase element describing mortar;  $R_{pas}$ —the ohmic resistance in pits or defects of passive layer;  $CPE_{pas}$ —the constant phase element for passive surface;  $R_{ct}$ —the charge transfer resistance;  $CPE_{dl}$ —constant phase element describing the double layer on the steel) [18].

The criteria for polarization data evaluation are given in [22] and [24].

### 3. Results and Discussion

All the obtained polarization curves have a course characteristic of steel in the passive state (Figure 3). In all cases, the gamma irradiation of the samples results in a shift of the corrosion potential values towards more negative potentials, indicating an increase in the probability of corrosion. The steel in all mortars is characterized by low  $j_{cor}$  values. However, only the non-irradiated mortars in cans in an environment with an RH = 50%  $j_{cor}$  value met the requirements for steel in the passive state ( $j_{cor} < 0.1 \mu\text{A}/\text{cm}^2$ ; negligible corrosion level). In other cases, the  $j_{cor}$  value indicates a low corrosion level. The corrosion current density increased after irradiation (Table 1), which means that the steel in irradiated mortars has a higher corrosion rate. In the case of samples stored in environment with 100% RH, gamma radiation caused a small increase in current density (1.1–1.3 times), while in the case of RH 50%, significantly higher  $j_{cor}$  values (4–12 times) for steel in irradiated samples were observed. The effect of RH on the course of the polarization curves of steel in irradiated mortars was small—the courses of polarization curves of steel in samples in environments with 50 and 100% RH were comparable. In contrast, in the case of non-irradiated samples, significantly lower values of  $j_{cor}$  and anodic current density were observed for 50% RH than for 100% RH. The highest values of  $j_{cor}$  and  $j_p$  were obtained for steel in mortar stored under laboratory conditions, which demonstrates the worst protective properties of the passive layer and the highest corrosion rate of steel. It may be related to the unrestricted access of  $\text{CO}_2$  to the samples stored in air, while other samples were sealed in cans.

**Table 1.** Characteristic parameters of polarization curves in plain mortars (50/100—RH value; ir—irradiated; can—in a can in a climatic chamber; air—laboratory conditions).

Parameters	air	50—can	50—ir	100—can	100—ir
$E_{cor}$ , V	−0.52	−0.25	−0.43	−0.31	−0.36
$j_{cor}$ , $\mu\text{A}/\text{cm}^2$	0.57	0.02	0.24	0.20	0.26
$E_p$ , V	−0.47	−0.19	−0.36	−0.25	−0.30
$j_p$ , $\mu\text{A}/\text{cm}^2$	13.9	0.6	4.4	3.8	5.0
$E_{tr}$ , V	0.55	0.57	0.55	0.54	0.54

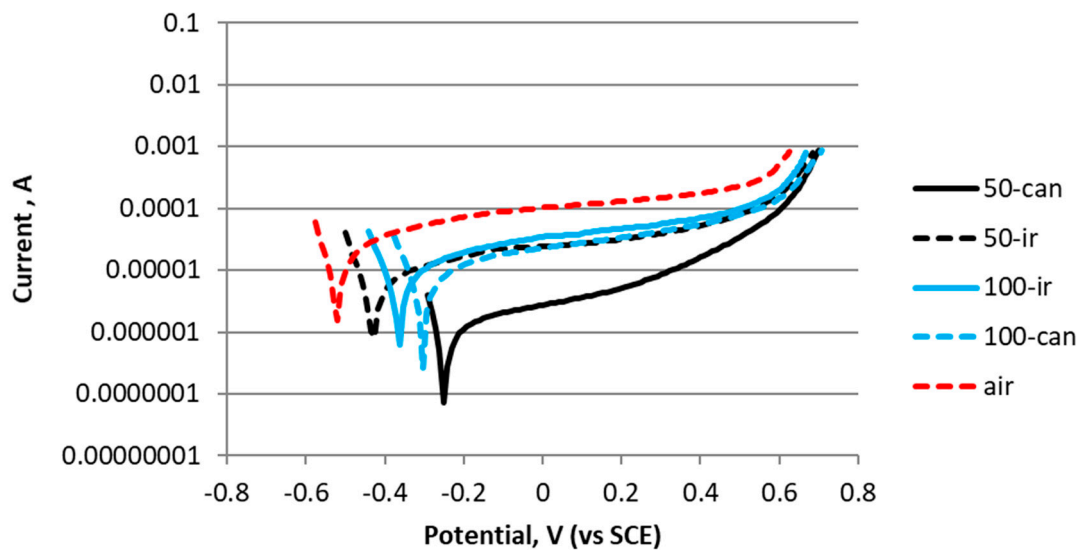


**Figure 3.** Polarization curves for steel rebar embedded in Portland cement mortar (50/100—RH value; ir—irradiated; can—in a can in a climatic chamber; air—laboratory conditions).

The characteristics of the steel in mortars on the Bode plots of the EIS spectra for samples conditioned under five different conditions are shown in Figure 4. The shape of the EIS spectra (wide phase angle peak) and high impedance at a low frequency indicates the presence of a passivation layer on the steel surface. The gamma radiation is responsible for shifting the impedance and phase angle to smaller values in the low frequency range. The above-mentioned effects are observed for all investigated specimens and indicate a deterioration in the quality of the passivation layer.

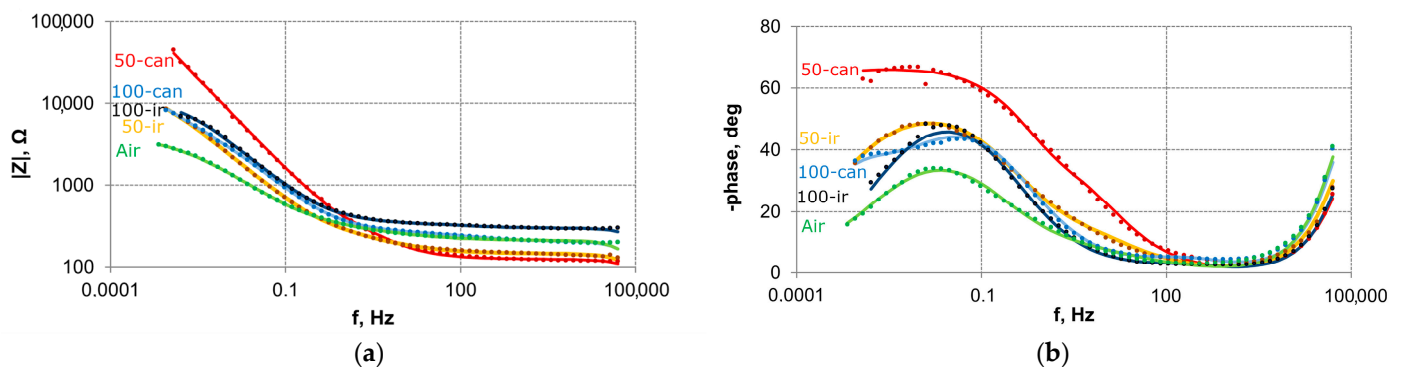


**Figure 4.** EIS spectra: (a) impedance, (b) phase shift for steel in mortars (points—measurement data; lines—fitting for equivalent circuit from Figure 2; 50/100—RH value; ir—irradiated; can—in a can in a climatic chamber; air—laboratory conditions).

The parameters determined on the basis of the equivalent circuit and the EIS measurement showed similar conclusions compared to polarization curve parameters (especially  $j_{\text{cor}}$ ). The polarization resistance  $R_p$  ( $R_{\text{ct}} + R_{\text{pas}}$ ) is the highest for the non-irradiated specimen at 50% RH (Table 2), which should be interpreted as the best protection of the passivation layer among the analysed specimens. In contrast, the smallest  $R_p$  values were present in mortar stored in air (air). The gamma irradiation of steel in mortar caused a decrease in  $R_p$  values—it was larger for RH = 50% than for RH = 100%—which indicates an acceleration of steel corrosion. It should be emphasized that the interpretation of changes takes place at a low level of steel corrosion. Increasing RH from 50% to 100% decreased  $R_p$  and therefore accelerated corrosion. It can be seen that the change in  $R_p$  due to an increase in RH was small for irradiated samples and significant for non-irradiated samples.

**Table 2.** Electrical circuit parameters for steel in mortar (50/100—RH value; ir—irradiated; can—in a can in a climatic chamber; air—laboratory conditions).

Parameters	air	50—can	50—ir	100—can	100—ir
$R_{pas}$ , $k\Omega \cdot cm^2$	1.56	5.15	2.12	0.38	0.48
$Y_{pas}$ , $\mu F s^{n-1} \cdot cm^{-2}$	132.0	50.5	111.0	2.4	20.1
$n_{pas}$	0.55	0.73	0.61	0.90	0.71
$R_{ct}$ , $k\Omega \cdot cm^2$	39	5010	204	207	122
$Y_{dl}$ , $\mu F s^{n-1} \cdot cm^{-2}$	201	43	122	173	146
$n_{dl}$	0.62	0.78	0.67	0.70	0.68

The gamma irradiation of mortars with steel bars caused a three-fold increase in capacity of the double layer ( $Y_{dl}$ ) compared to non-irradiated specimens stored under 50% RH conditions. The physical interpretation of such a determination is an increasing thickness of the electrical double layer and consequently loses the stability of the passivation layer and iron dissolution [25]. In the case of fully saturated mortar (RH-100), the opposite relationship was observed— $Y_{dl}$  after gamma irradiation decreased by about 15–30%. A 15% decrease in the  $n$  parameter is also observed for steel in mortar at 50% and exposure to gamma radiation. This effect is due to the reduced uniformity of the passive layer on steel, and thus a degradation of its protective properties. In the case of RH-100 mortar, no effect of gamma radiation on the  $n$  parameter was observed.

#### 4. Conclusions

The electrochemical parameters of steel rods in mortar conditioning in specific environmental conditions (the dose of gamma radiation reached 1.8 MGy and environmental conditions favoured the progress of carbonation phenomena) result in the following conclusions:

1. The increasing RH from 50% to 100% resulted in the intensification of the deterioration of the protective properties of the passive layer on the steel and the accelerated corrosion of the steel in non-irradiated specimens. The effect of gamma radiation on the corrosion of steel in the mortar is significantly greater in an atmosphere of 1% CO<sub>2</sub> and moderate RH (50%) than 1% CO<sub>2</sub> and fully saturated conditions (RH = 100%);
2. Steel in mortar stored in closed, low-volume cans had a better passive layer and lower corrosion rate than steel in mortar stored in a laboratory atmosphere.

**Author Contributions:** Conceptualization, M.D.; methodology, M.D. and M.A.G.; validation, M.D.; formal analysis, M.A.G.; investigation, M.D., J.K., K.D.; data curation, M.D. and J.K.; writing—original draft preparation, M.D.; writing—review and editing, M.D., J.K.; visualization, M.D. and J.K.; supervision, M.A.G.; project administration, M.A.G.; funding acquisition, M.A.G. All authors have read and agreed to the published version of the manuscript.

**Funding:** This research was funded by the National Centre for Research and Development, Poland, grant number Project V4-Korea/2/2018.

**Institutional Review Board Statement:** Not applicable.

**Informed Consent Statement:** Not applicable.

**Data Availability Statement:** Not applicable.

**Acknowledgments:** Publication cost of this paper was covered with funds of the Polish National Agency for Academic Exchange (NAWA): “MATBUD’2023—Developing international scientific cooperation in the field of building materials engineering” BPI/WTP/2021/1/00002, MATBUD’2023

**Conflicts of Interest:** The authors declare no conflict of interest.

## References

1. Tchnerer, J.; Vaithilingam, L.; Han, M. Effective aging management of NPP concrete structures. *J. Adv. Concr. Technol.* **2017**, *15*, 1–9. [[CrossRef](#)]
2. Lindqvist, J.A.; Flansbjerg, M.; Hansson, E. *Analysis of Irradiated Concrete*; Report 2016:239; Energiforsk: Stockholm, Sweden, 2016.
3. Field, K.G.; Remec, I.; Le Pape, Y. Radiation effects in concrete for nuclear power plants—Part I: Quantification of radiation exposure and radiation effects. *Nucl. Eng. Des.* **2015**, *282*, 126–143. [[CrossRef](#)]
4. Soo, P.; Milian, L.M. The effect of gamma radiation on the strength of Portland cement mortars. *J. Mater. Sci. Lett.* **2001**, *20*, 1345–1348. [[CrossRef](#)]
5. Robira, M.; Hilloulin, B.; Loukili, A.; Potin, G.; Bourbon, X.; Abdelouas, A. Multi-scale investigation of the effect of  $\gamma$  irradiations on the mechanical properties of cementitious materials. *Constr. Build. Mater.* **2018**, *186*, 484–494. [[CrossRef](#)]
6. Mobasher, N.; Bernal, S.; Kinoshita, H.; Sharrad, C.; Provis, J. Gamma irradiation resistance of an early age slag-blended cement matrix for nuclear waste encapsulation. *J. Mater. Res.* **2015**, *30*, 1563–1571. [[CrossRef](#)]
7. Glinicki, M.A.; Dąbrowski, M.; Antolik, A.; Dziedzic, K.; Sikorin, S.; Fateev, V.; Povolansky, E. Gamma irradiation sensitivity of early hardening cement mortar. *Cem. Concr. Compos.* **2022**, *126*, 104327. [[CrossRef](#)]
8. Dąbrowski, M.; Glinicki, M.A.; Dziedzic, K.; Józwiak-Niedźwiedzka, D.; Sikorin, S.; Fateev, V.S.; Povalansky, E.I. Early age hardening of concrete with heavy aggregate in gamma radiation source—Impact on the modulus of elasticity and microstructural features. *J. Adv. Concr. Technol.* **2021**, *19*, 555–570. [[CrossRef](#)]
9. Maruyama, I.; Ishikawa, S.; Yasukouchi, J.; Sawada, S.; Kurihara, R.; Takizawa, M.; Kontani, O. Impact of gamma-ray irradiation on hardened white Portland cement pastes exposed to atmosphere. *Cem. Concr. Res.* **2018**, *108*, 59–71. [[CrossRef](#)]
10. Potts, A.; Butcher, E.; Cann, G.; Leay, L. Long term effects of gamma irradiation on in-service concrete structures. *J. Nucl. Mater.* **2021**, *548*, 152868. [[CrossRef](#)]
11. Rasheed, P.A.; Nayar, S.K.; Barsoum, I.; Alfantazi, A. Degradation of Concrete Structures in Nuclear Power Plants: A Review of the Major Causes and Possible Preventive Measures. *Energies* **2022**, *15*, 8011. [[CrossRef](#)]
12. Reches, Y. A multi-scale review of the effects of gamma radiation on concrete. *Results Mater.* **2019**, *2*, 100039. [[CrossRef](#)]
13. Jaśniok, M.; Jaśniok, T. Measurements on corrosion rate of reinforcing steel under various environmental conditions, using an insulator to delimit the polarized area. *Procedia Eng.* **2017**, *193*, 431–438. [[CrossRef](#)]
14. Macdonald, D.D.; Engelhardt, G.R.; Petrov, A. A Critical Review of Radiolysis Issues in Water-Cooled Fission and Fusion Reactors: Part I, Assessment of Radiolysis Model. *Corros. Mater. Degrad.* **2022**, *3*, 470–535. [[CrossRef](#)]
15. Aljohania, T.A.; Geesib, M.H.; Kaibac, A.; Al-Mayouf, A.M.; Khoshnaw, F. Characterization of gamma-ray irradiation influence on the corrosion behaviour of austenitic stainless steel. *Mater. Today Commun.* **2020**, *24*, 101242. [[CrossRef](#)]
16. Liu, C.; Wang, J.; Zhang, Z.; Han, E.-H.; Liu, W.; Liang, D.; Yang, Z.; Cao, X. Effect of cumulative gamma irradiation on microstructure and corrosion behaviour of X65 low carbon steel. *J. Mater. Sci. Technol.* **2018**, *34*, 2131–2139. [[CrossRef](#)]
17. Dewynter-Marty, V.; Chomat, L.; Guillot, W.; Amblard, E.; Durand, D.; Cornaton, M.; Bourbon, X. Concrete radiolysis effect on steels corrosion and comparison with non-irradiated material. In Proceedings of the EUROCORR 2017—20th International Corrosion Congress/Process Safety Congress 2017, Prague, Czech Republic, 3–7 September 2017.
18. Dąbrowski, M.; Glinicki, M.A.; Kuziak, J.; Józwiak-Niedźwiedzka, D.; Dziedzic, K. Effects of 2 MGy gamma irradiation on the steel corrosion in cement-based composites. *Constr. Build. Mater.* **2022**, *342*, 127967. [[CrossRef](#)]
19. EN 197-1:2012; Cement: Composition, Specifications and Conformity Criteria for Common Cements. European Committee for Standardization: Brussels, Belgium, 2012.
20. EN 196-1:2016; Methods of Testing Cement: Determination of Strength. European Committee for Standardization: Brussels, Belgium, 2016.
21. EN 10025-2:2019; Hot Rolled Products of Structural Steels Part 2: Technical Delivery Conditions for Non-Alloy Structural Steels. European Committee for Standardization: Brussels, Belgium, 2019.
22. PN-B-01810:1986; Protection Against Corrosion in Building—Protective Properties of Concrete Referring to Reinforcing Steel—Electrochemical Tests. Polish Committee for Standardization: Brussels, Belgium, 1986. (In Polish)
23. Józwiak-Niedźwiedzka, D.; Dąbrowski, M.; Dziedzic, K.; Jarząbek, D.; Antolik, A.; Denis, P.; Glinicki, M.A. Effect of gamma irradiation on the mechanical properties of carbonation reaction products in mortar. *Mater. Struct.* **2022**, *55*, 164. [[CrossRef](#)]
24. Andrade, C.; Alonso, C.; Gulikers, J.; Polder, R.; Cigna, R.; Vennesland, Ø.; Salta, M.; Raharinaivo, A.; Elsener, B. RILEM TC 154-EMC: Electrochemical Techniques for Measuring Metallic Corrosion. Recommendations. Test methods for on-site corrosion rate measurement of steel reinforcement in concrete by means of the polarization resistance method. *Mater. Struct.* **2004**, *37*, 623–643. [[CrossRef](#)]
25. Montemor, M.F.; Cunha, M.P.; Ferreira, M.G.; Simoes, A.M. Corrosion behaviour of rebars in fly ash mortar exposed to carbon dioxide and chlorides. *Cem. Concr. Compos.* **2002**, *24*, 45–53. [[CrossRef](#)]

**Disclaimer/Publisher’s Note:** The statements, opinions and data contained in all publications are solely those of the individual author(s) and contributor(s) and not of MDPI and/or the editor(s). MDPI and/or the editor(s) disclaim responsibility for any injury to people or property resulting from any ideas, methods, instructions or products referred to in the content.